Paulina Sawicka-Chudy
Department of Biophysics, Faculty of Mathematics and Natural Sciences, University of Rzeszow
Pigonia 1, 35-317 Rzeszow, Poland, sawicka61@wp.pl

Maciej Sibiński
Department of Semiconductor and Optoelectronics, Lodz University of Technology
Wólczańska 211/215, 90-924 Lodz, Poland

Marian Cholewa
Department of Biophysics, Faculty of Mathematics and Natural Sciences, University of Rzeszow
Pigonia 1, 35-317 Rzeszow, Poland

Maciej Klein
**Centre for Plasma and Laser Engineering, The Szewalski Institute of Fluid-Flow Machinery,
Polish Academy of Science**
Fiszera 14, 80-231 Gdansk, Poland
Faculty of Applied Physics and Mathematics, Gdansk University of Technology
Narutowicza 11/12, 80-233 Gdansk, Poland

Katarzyna Znajdek
Department of Semiconductor and Optoelectronics, Lodz University of Technology
Wólczańska 211/215, 90-924 Lodz, Poland

Adam Cenian
**Centre for Plasma and Laser Engineering, The Szewalski Institute of Fluid-Flow Machinery,
Polish Academy of Science**
Fiszera 14, 80-231 Gdansk, Poland

TESTS AND THEORETICAL ANALYSIS OF A PVT HYBRID COLLECTOR OPERATING UNDER VARIOUS INSOLATION CONDITIONS

Abstract

The main goal of the study was to investigate the relationship between the orientation of the PVT (PhotoVoltaic Thermal) collector and the thermal and electric power generated. Extensive research was performed to find optimal tilt angles for hybrid solar thermal collectors, which combine photovoltaic as well as thermal collection in a single unit, known as PVT (PhotoVoltaic Thermal) modules for an office building with working hours between 7.00 and 16.00. The comprehensive study included field measurements of the modules in central Poland and tests under AM (air mass) 1.5 conditions in a certified laboratory KEZO (Centre for Energy Conversion and Renewable Resources) Polish Academy of Sciences in Jablonna. Furthermore, a PVT system was investigated using the simulation method based on the dedicated *Polysun* software. The PV characteristics and efficiency of the PV module and the relation between power or efficiency of the PVT module and incidence angle of solar-irradiance were studied. Optimal work conditions for commercial PVT modules were ascertained. In addition, it was found that the maximum efficiencies of PV module (η_{PV}), solar thermal-collector (η_c) and PVT hybrid collector (η_{PVT}) registered under field conditions were higher than the ones measured under laboratory conditions.

Key words
Conversion of solar energy, Photovoltaics, Silicon solar cells, PVT collector.

Introduction
Energy plays a vital role in daily human needs. Worldwide, energy consumption has shown rapid growth, which is the important global energy problem. PV modules generate clean electricity, reducing air pollution and having only little environmental impact. Now, typical efficiency of PV modules is in the range 15%÷20% [1]. The conversion of solar energy into electric power depends on the location, orientation, and type of photovoltaic

(PV) system. PVT hybrid collector works with even higher efficiency than sum of the solar thermal collector and PV module efficiencies [2] and simultaneously produces electrical and thermal power. The thermal efficiency of the flat-plate thermal collector is 40–60%. Therefore, the estimated efficiency of the PVT collector is the range from 60 to 80% [3]. In 1979 the first PVT model was demonstrated in Ref. [4]. Until now the PVT systems have been studied from various aspects: system design, performance analysis, simulation models, field or indoor experimental validation, economic and cost-effective analysis [2, 5-8]. Coventry [9] has developed and tested a PVT with a geometric concentration ratio of 37. Chow et al. [10] developed a prototype thermosyphon PVT collector made of aluminum alloy flat box. Dupeyrat et al. [11] tested the design of a prototype single glazed flat plate PVT collector focusing on the heat transfer between PV cells and fluid [3].

Nevertheless PVT hybrid collectors presents numerous advantages, specific work conditions and often contradictory requirements of both technologies cause extensive need for further technology investigation. Considering above facts, this paper aims on to studies of the relationship between orientation of PVT collectors and their thermal and electric power generation. Extensive research was performed to determine the optimal working angle for practical PVT installations. The parameters of the PVT system were measured in field and laboratory conditions. The results were confirmed using specialized computer program Polysun. Acquired results are useful for the design and construction of functional PVT systems.

1. Description of experiments

The research subject was a commercially available photovoltaic thermal hybrid solar collector manufactured by Volther Power Therm measuring 1640 x 870 x 105 mm. Fig. 1 presents the operation parameters of the collector for STC (Standard Test Conditions) [12].

Parameter	Value
Absorber type (PV)	Mono-crystalline
Absorber surface (T)	Copper
Nominal current I_{mp}	5.43 A
Short circuit current I_{sc}	5.67 A
Nominal voltage V_{mp}	36.8 V
Open circuit voltage V_{oc}	45.43 V
Cell efficiency	18%
Collector area	1.4 m^2
Nominal power	200 W
Efficiency (absorber)	49%
Peak power (at 1000 W/m^2)	680 W
Capacity	1.2 dm^3

Fig. 1. Outlook and parameters of investigated PVT collectors.
Source: Author's

Initial studies were performed under field conditions. Field experiments were conducted at the Technology Transfer Centre for Renewable Energy in Lodz (Φ = 51° 44' N, ϕ = 19° 21' E). The PVT hybrid collectors were located on the roof of the building and were inclined at 30º from the horizontal axis in a southern orientation: (E = +90°, S = 0°, W = -90°). Figure 2 presents a schematic diagram of the installation.

Research was done during the autumnal equinox at the beginning of October, during daytime between 8.00 and 16.00. It is assumed that the results obtained at the equinox will correspond well to the annual average values. The weather station on the roof of the building allowed determination of the meteorological conditions.
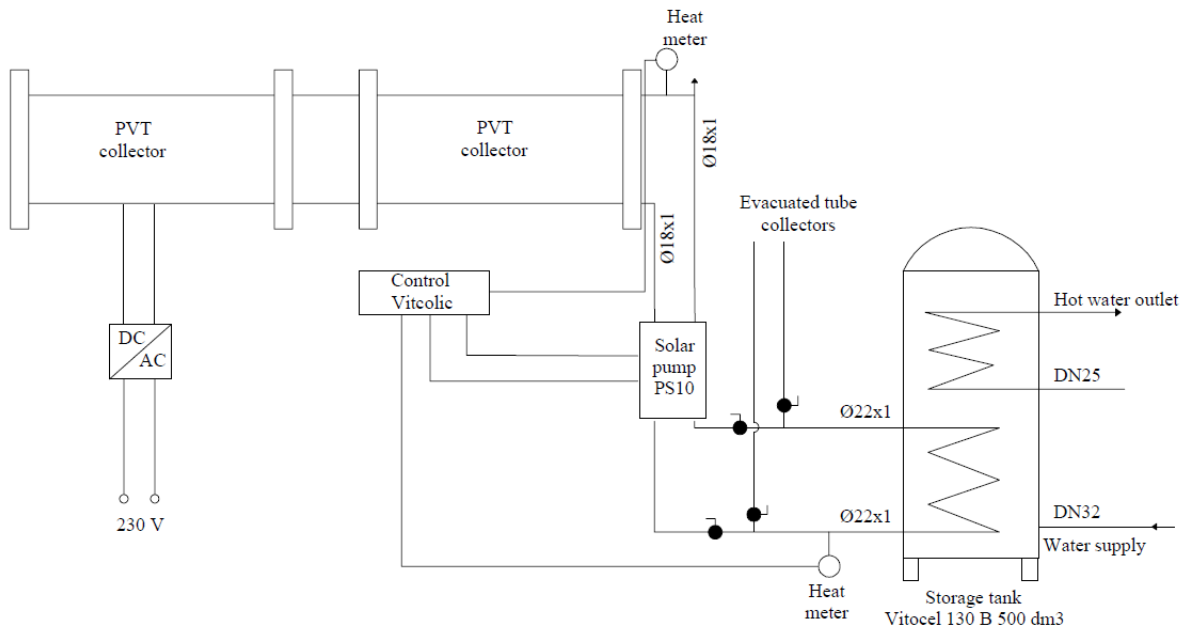
Fig. 2. Schematic diagram of installation PVT collectors.
Source: Author's

Figures 3 presents weather conditions on 2 October 2015 (solar irradiance on a horizontal surface, I_{rr} (right axis), solar elevation (it is the angle between the direction of the geometric center of the Sun and the horizon), S_e [13], the solar altitude angle (it is the angle between solar radiation which falls for receiver and receiver) for positioning the receiver at angles of 30° $S_{a30º}$ and 60º $S_{a60º}$ (left axis). Table 1 shows ambient temperature, T_a, wind speed, v, and values of solar elevation, S_e.
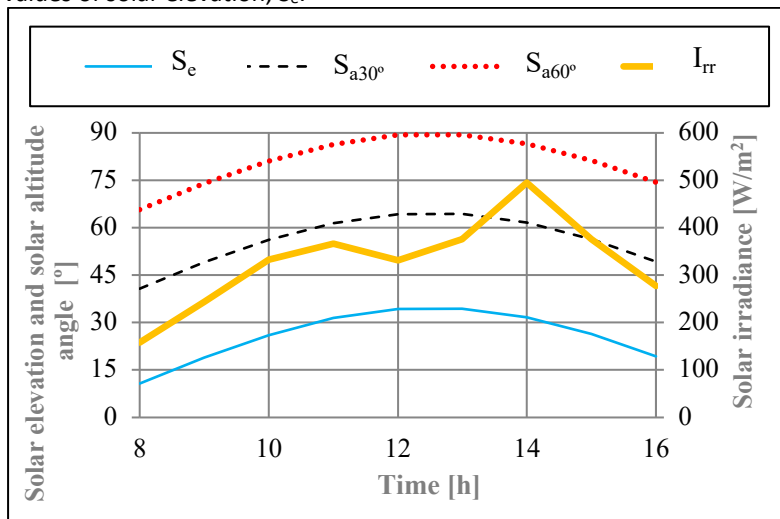

Fig. 3. The solar irradiance measured during field experiment, solar elevation and calculated solar altitude angle.
Source: Author's

Table 1. Ambient temperature, wind speed, values of solar elevation on 2 October 2015.

Time	T_a [ºC]	S_e [º]	v [m/s]
8.00	4.3	10.73	1.1
9.00	5.3	19.03	2.4
10.00	10.8	26.10	2.2
11.00	13.9	31.42	2.0
12.00	15.8	34.33	3.0
13.00	17.4	34.39	2.2
14.00	19.3	31.60	2.9
15.00	19.4	26.38	2.4
16.00	20.3	19.33	2.1
The average	14.07	–	2.3

Source: Author's

All electrical data were determined using a multifunction I-V Curve Tracer (HT IV 400). The acquired data included voltage-current characteristics (I-V curve), maximum power point (MPP) and power at MPP (P_{max}), the current ($I_{mp,}$ accuracy ±0.5%) and voltage ($V_{mp,}$ uncertainty ±0.5%) at maximum power point, the short circuit current (I_{sc}) and the open circuit voltage (V_{oc}) - see I-V curves at various module temperatures at Fig. 11a in Appendix. Solar irradiance was determined using a pyranometer SP Lite2 KIPP& ZONEN (uncertainty ±0.05%). Solar circuit systems was control by solar controller VI ECO SOL 200 (uncertainty ±1ºC).

Later, PVT tests were conducted under laboratory conditions. Clean water was used as a solar working fluid. The photovoltaic characteristics of the PVT module were measured under STC conditions using a class AAA steady-state solar simulator (LA150200, Eternal Sun) equipped with an AM 1.5 G filter. The light intensity was determined by a silicon reference cell (ReRa Solutions) and corrected to 1000 W/m^2. I-V curves were recorded on IV-System Pro (ReRa Solutions) and a Tracer IV-curve software (ReRa Solutions). The IV-System Pro consist of an EL 9000A (Elektro Automatik) electronic DC load connected with two 34410A (Agilent) multimeters, for PV panels measurements, and a 2401 SourceMeter Keithley (uncertainty ±0.012%), for I-V measurements of a reference cell. During measurements the temperature difference between the inlet fluid and the ambient air was set to: ΔT = 5 K and ΔT = 30 K. Temperatures were measured by PT100 (class A, uncertainty ±0,15 °C) temperature sensors connected to a 34970A (Agilent) data acquisition control unit. Afterwards, solar thermal collector tests were carried out. During measurements, in order to better reflect the natural conditions, the solar simulator was operated in ST1000 mode wherein infrared radiation intensity is higher. Therefore, the light intensity was determined using an IR02 pyrgeometer Hukseflux (uncertainty ±15 °C) and a SR11 pyranometer Hukseflux (uncertainty ±8%) connected to a 34970A (Agilent) data acquisition control unit. The mass flow rate of fluid through the solar thermal collector was set to 1.3 kg/min and was determined by an Optimass 6400 C Krohne (uncertainty ±0.1%) mass flow meter.

2. Model description

The measured energy characteristics and the PVT system efficiency were verified using the *Polysun* software from the company VELA SOLARIS [14]. This part is mostly for comparative and demonstration use rather than for reliably justified conclusions, as the applied meteorological conditions do not refer to the specific test localization (due to known limitation regarding the license of this software version). The program provides dynamic simulations of thermal, photovoltaic and PVT systems and enables their optimization [16]. *Polysun* 8.1. Simulation Software Designer Demo is available now [14]. For prediction or estimation of efficiency of PVT collector (ε_{sys}) the following equation is considered in this study [15]:

$$\varepsilon_{sys} = (Q_{use} + E_{inv})/(E_{aux} + E_{par}), \% \tag{1}$$

where Q_{use} is the effective energy consumption [kWh], E_{inv} is energy supplied to the grid from the inverter [kWh], E_{aux} is auxiliary energy, E_{par} is parasitic energy of the respective system [kWh].

The parameters of the PVT system used in our simulations are listed down in Table 2.

Table 2. The parameters values of PVT system.

Parameters	Value
Number of residents	4
Orientation of PVT collectors	South
Number of PVT modules	6
System specification	Commercial system
Hydronic system template	Hybrid Solar PV and solar hot water residential 1 tank system
Auxiliary heating	Oil

Source: Author's

The setup of the solar PVT system used in this research is depicted in Figure 4. On the left side of the picture is the PVT collector, and in the center is the APU (auxiliary power unit). Both components are connected to the heat exchangers. Number of PVT modules was dedicated by program *Polysun* for 4 residents.
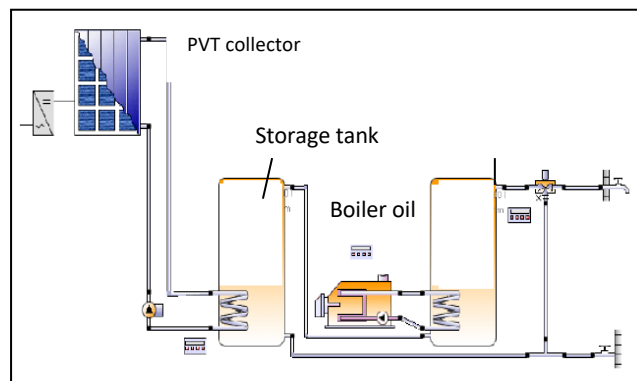
Fig. 4. A solar PVT system designed using Polysun program.
Source: Author's

3. Results and discussion
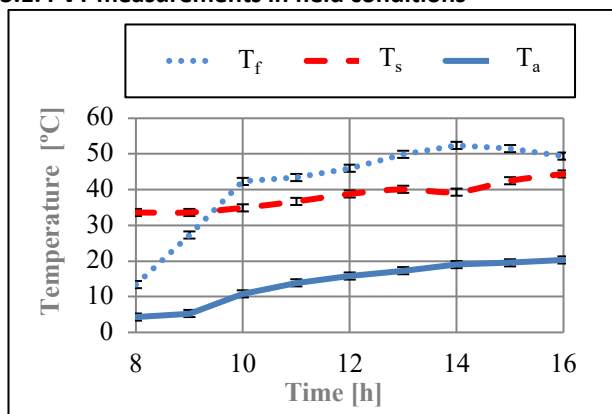### 3.1. PVT measurements in field conditions

Fig. 5a. Field test results of ambient temperature, the fluid temperature at the collector outlet, and the water temperature in the storage tank during daylight operation time.
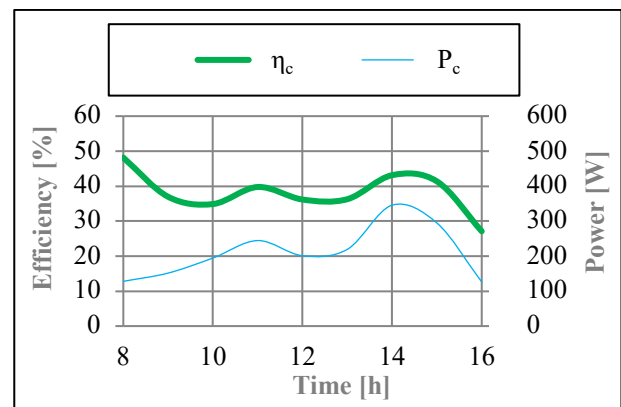*Source: Author's*

Fig. 5b. Instantaneous power and efficiency values of solar thermal collector.
Source: Author's

Initially, measurements related to thermal-collector operation were performed under field conditions (described in Figures 3). Performance data was not STC-corrected. Authors showed "raw" data to analyzed real work of PVT

system. Figure 5a summarizes the data related to the temperatures of ambient air (T_a), of the cooling water at the collector outlet (T_f) and of water in the storage tank (T_s). The daytime operation of a solar thermal collector can be divided into two periods. First, between 8.00 and 10.00, the cooling water temperature of the solar thermal collector, T_f, rises from 13 to 42ºC. At that moment, a circulation pump is activated leading to a heat exchange between water from the heat collector and water in the storage tank (see red curve in Fig. 5a). The temperature of the water in the storage tank, T_s, slowly increases but the temperature of the water in the collector holds steady for one hour (see plateau on T_f curve). Later, between 11.00 and 14.00 the water temperature in the collector increases quasi linearly. Although the temperature T_f decreases after 14.00 due to a strong decrease of solar irradiance and heat exchange with colder water in storage tank, the heat energy collected at the storage tank increases even after 16.00. At 16.00 the controller turns off the circulation pump to prevent possible heat losses from the water in the storage tank. The temperature difference of water collected in the solar collector and water in the storage tank approaches "zero" and later goes negative. The thermal heat energy accumulated in the storage tank (Q) was ~ 10 MJ. It can be calculated using the measured temperatures and model described in Ref. [16] given by the following equation:

$$Q = V\rho k_c(T_z - T_p), [J] \tag{2}$$

where V is the fluid capacity flow rate during the day (m^3), ρ is density (kg/m^3), k_c is the heat capacity of water $J/(kg \cdot K)$, T_z is the inlet fluid temperature to storage tank (K), T_p is the outlet fluid temperature to the storage tank (K).

Figure 6b shows the instantaneous power (P_c) and efficiency (η_c) of the thermal collector calculated using the model [17]. The power P_c is given by the following equation:

$$P_c = A_c[\beta\tau I_{rr} - k(T_{ab} - T_a)], [W], \tag{3}$$

where A_c is total collector aperture area (m^2), $\beta\tau$ is transmittance–absorptance product, k is solar-collector heat-transfer loss-coefficient ($W/m^2 \cdot ºC$), T_{ab} is average temperature of the absorbing surface (ºC), T_a is ambient temperature (ºC), I_{rr} is instantaneous solar irradiance (W/m^2).

The PV electric performance was also studied. Figure 6a shows how the module electric parameters (I_{mp}, V_{mp}) at maximum power point changes during the chosen day. The interrelation between the instantaneous solar irradiance (I_{rr}) and instantaneous, PV power at MPP (P_{max}) and efficiency (η_{PV}) is shown in Figure 7b.
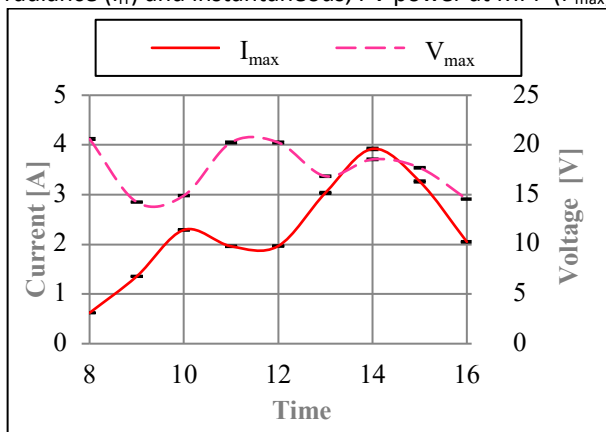

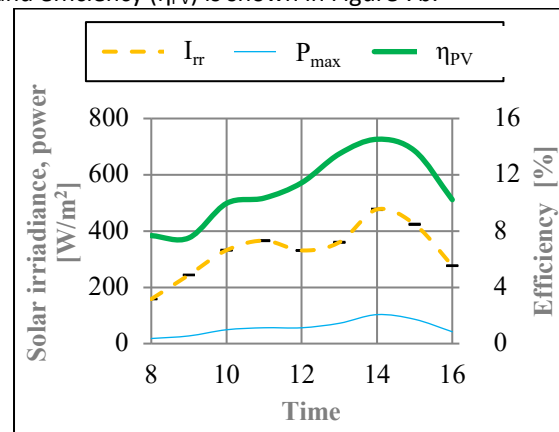Fig. 6a. Current and Voltage at MPP of PV module.
Source: Author's

Fig. 6b. P_{max}, I_{rr}, η_{PV} values of PV panel.
Source: Author's

Figure 6a shows that the I_{mp} current strongly depends on irradiance (compare with I_{rr} at Fig. 6b), while voltage varies in a small range 14÷21 V. The black lines represent error bars. The PV current in the range 0.8÷ 3.9 A was measured. As solar irradiance increases three times, the current grows ~400%. Figure 7b shows that as the solar irradiance increases, the values of P_{max} and η_{PV} also increase. The instantaneous efficiency was found in the range from about 8% (morning hours, S_e = 10.73º) to 14% (irradiation about 600 W/m^2, S_e = 33.14º). The amount of power generated and voltage by PVT system was consistent with the solar irradiance. The maximum values were achieved at 14.00. The electric energy production-density, 475 Wh/m^2, was determined using formula in Ref. [18]. The instantaneous maximum output-power MPP, 143 W (S_e = 33.14º) was about 28% lower than the nominal power of the PV module (200 W).

3.2. PVT tests under laboratory conditions

The relation of PVT module performance and solar-simulator altitude-angle were investigated under laboratory conditions. First, the PV module and later thermal collector performance was studied.

Impact of solar-simulator altitude-angles on performance of PV module and thermal collector

The photovoltaic electric characteristics were measured for different solar-simulator altitude-angles α and temperature difference ΔT = 5ºC and ΔT = 30ºC (between the temperature of water at the inlet to thermal collector and the ambient air). The light intensity was adjusted to 1000 W/m^2. The altitude angle was varied between 30 º and 90º (for 90º the solar simulator was situated parallel to the PVT module).
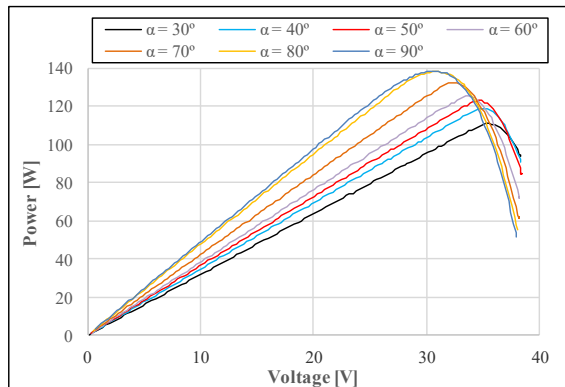

Fig. 7a. The P–V characteristics of PV module for different angles of radiation incidence for ΔT = 5ºC.
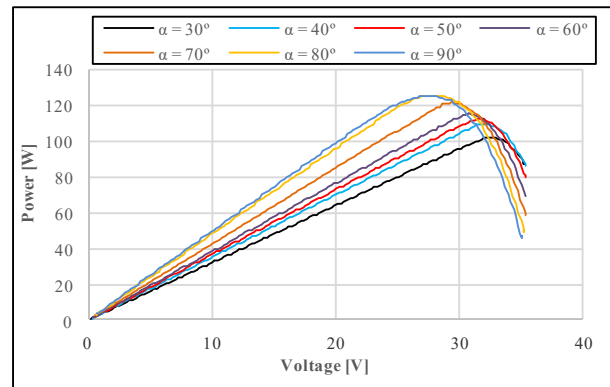*Source: Author's*

Fig. 7b. The P–V characteristics of PV module for different angles of radiation incidence for ΔT = 30ºC.
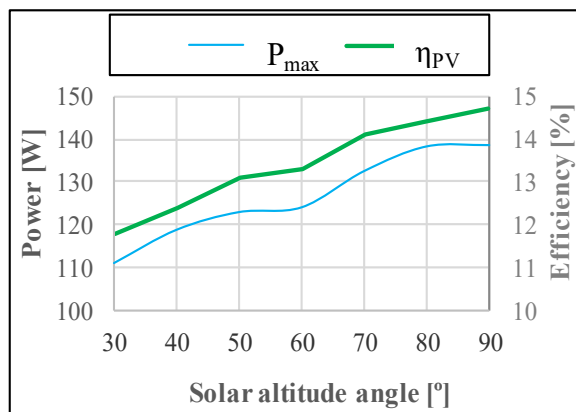*Source: Author's*

Fig. 8a. The power (P$_{max}$) and efficiency (η$_{PV}$) as function of altitude angle for ΔT = 5ºC.
Source: Author's
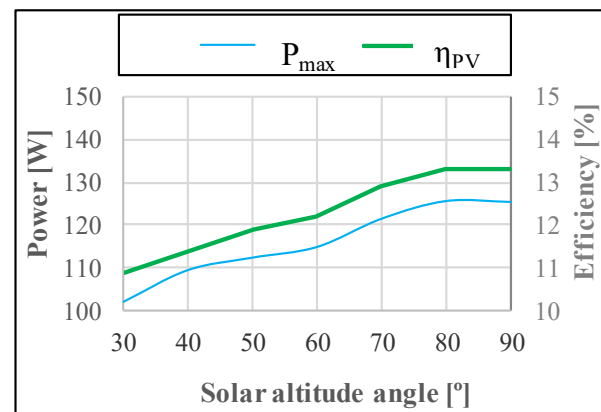
Fig. 8b The power (P$_{max}$) and efficiency (η$_{PV}$) as function of altitude angle for ΔT = 30ºC.
Source: Author's

Figures 8a and 8b show that the PV power at MPP and efficiency increases when the solar altitude angle increases, both for ΔT = 5°C and 30°C. As the temperature difference ΔT rises from 5 to 30°C the power at MPP, P$_{max}$, decreases about 7 W. The maximum value of P$_{max}$ was registered for α = 80-90°; it was 138 W (at V$_{mp}$ ~ 32V) and 125 W (V$_{mp}$ ~27V), for ΔT = 5 and 30°C, respectively. As altitude angle, α, decreases P$_{max}$ decreases but V$_{mp}$ increases (from 32 to 36V) for ΔT= 5°C. The open circuit Voltage, Voc, increases as well. The dip at 60º could be caused by absorption and reflection.
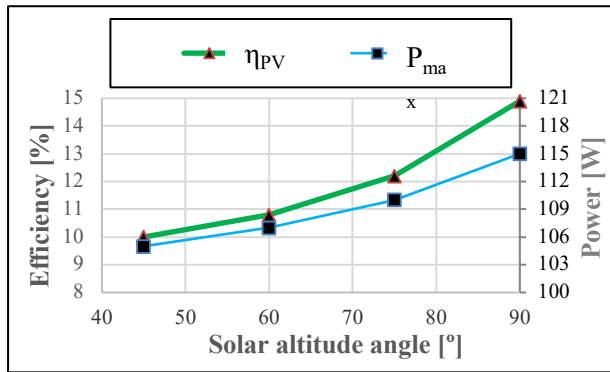
Fig. 8c. The power (P$_{max}$) and efficiency (η$_{PV}$) as function of altitude angle for ΔT = 10ºC.
Source: Author's

Then, the PV module and the solar thermal collector were also studied for ΔT = 10ºC. Figure 9c shows that the PV power at MPP and efficiency increases when the solar altitude angle increases, from 104 to 115 W and 10 to 15%, respectively.

The performance of the thermal part of PVT and its dependence on solar-altitude angles was also investigated. The relation between instantaneous thermal power of solar collector (P$_c$) calculated based on eq. (3), (as well as efficiency) and the solar altitude angle was studied (see results in Table 3 and Figure 9). Table 3 shows solar-simulator irradiance and measured difference between cooling fluid temperature at the collector outlet and at the inlet (T$_{outlet}$ -T$_{inlet}$) as function of the solar-altitude angle. As the solar-altitude angle increases from 45-75° the temperature difference, T$_{outlet}$ -T$_{inlet}$, falls 3 times (from 0.64 to 0.21 K). As the altitude angle of the solar simulator increases, solar irradiance and the solar collector output-power also increase.

The efficiency (in contrast to power) of the thermal collector varies differently in relation to the solar altitude angle; it decreases slightly and then increases with the solar altitude angle following the tendency of T$_{outlet}$ -T$_{inlet}$. Moreover, the efficiency drops only ~6%, whilst power increases by 75% of initial value (Fig. 9). This is important for electric-thermal power balancing under real installation conditions.
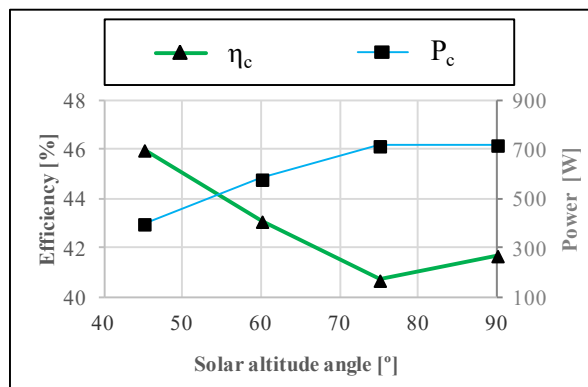

Fig. 9. Power output and total efficiency as function of solar-altitude angle for solar thermal collector for ΔT =10ºC.
Source: Author's

Table. 3. Interrelation between the solar altitude angle, irradiance and T$_{outlet}$ -T$_{inlet}$.

Solar altitude angle [º]	Irradiance [W/m²]	T$_{outlet}$ -T$_{inlet}$ [K]
45	588	0.64
60	937	0.59
75	1204	0.21
90	1225	0.48

Source: Author's

4. Comparison of results

The efficiency of PVT (η_{PVT}) collectors under both field (during the autumnal equinox) and laboratory conditions as a function of the solar-altitude angle was calculated using equation [19]:

$$\eta_{PVT} = \eta_{PV} + \eta_c \qquad . \tag{4}$$

In the case of the field experiment, the values of efficiency for the thermal collector (η_c) (see Figure 10a) were deduced from data presented in Figure 6b, where the solar-altitude angle as a function of time was determined using the data shown in Figure 3 for a module positioned under 30° angle ($S_{a30º}$). The same was done for efficiency of PV module (η_{PV}) under field conditions, but this time using the data presented in Figure 6b. The rather erratic character of the field experiment data should be related to changing weather conditions, such as wind and air temperature. The variation of the solar altitude angle is limited to range 40-65º achievable for the chosen position of the solar panel during the autumnal equinox.

In the case of the laboratory experiment, the efficiency of the thermal collector (presented in Figure 10b) was assumed from the data presented in Figure 10c. The values of PV module efficiency were derived from the data presented in Figure 10, as ~ΔT = 10ºC was observed during the field experiment.
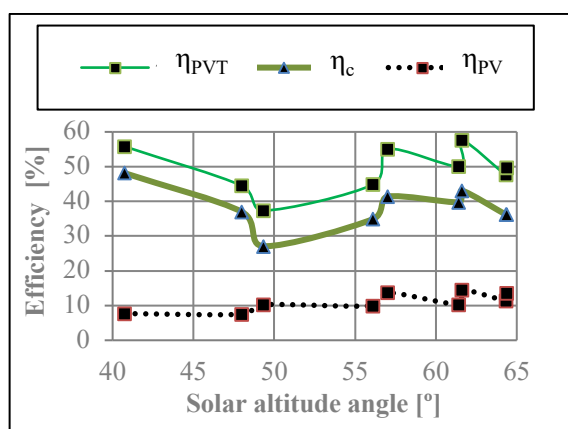

Fig. 10a. Efficiency measured under field conditions.
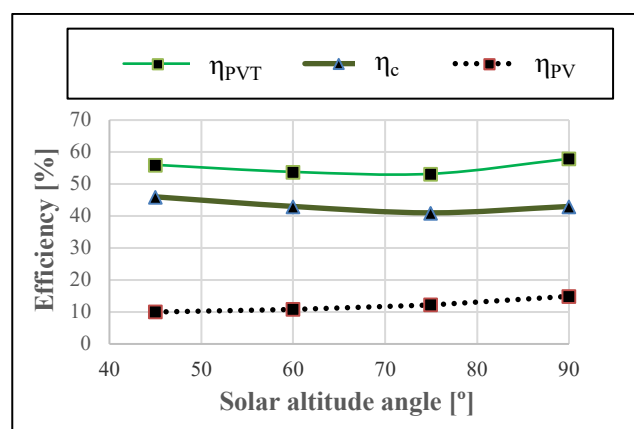*Source: Author's*

Fig. 10b. Efficiency measured under laboratory conditions.
Source: Author's

The calculated maximum values of η_{PV}, η_c and η_{PVT} efficiencies and optimal (i.e. corresponding to the maximum value) solar altitude angle, α, for a PVT collector are shown at Table 4. It should be underlined that the values of PVT efficiency do not vary much under laboratory conditions and are close to the maximal values under field conditions. Generally good agreement between the maximal values of efficiencies can be observed, however significant difference in the optimal tilt angle needs to be investigated and addressed in the future. The optimal value of the solar altitude angle for η_c is the smallest considered in this study, both under field and laboratory conditions. In both cases, the PV efficiency grows with α. We recalculated altitude angle to the tilt angle (it is the angle between receiver and horizontal position) to compare results in literature. In the literature there are only tilt angle of receivers. The results are in agreement with the earlier reported works [20].

Table 4. Maximum efficiency of PV module (η_{PV}), solar thermal-collector (η_c) and PVT hybrid collector (η_{PVT}) as well as related optimum solar altitude-angles measured.

	Maximum efficiency (respective solar altitude angle)	
	Field conditions	**Laboratory conditions**
η_{PV}	14.5% (62º)	14.9% (90º)
η_c	48.0% (40º)	46.0% (45º)
η_{PVT}	57.7% (62º)	57.9% (90º)

Source: Author's

Calculated values of PVT collector efficiency (η_{PVT}) were compared with the values obtained from the computer program *Polysun* for *the period* during the autumnal equinox at 12.00 for solar altitude angles in the range 45 - 90º. The PVT module efficiency reaches its maximum at α = 90º; the results under laboratory conditions show a similar tendency, although this is screened by oscillations due to weather conditions (e.g. wind and rain). This fact indicates the need for longer-term outdoor observation, necessary for temporary disturbances elimination Nevertheless one may confirm that, the simulated values do not vary much in the range of the considered solar altitude angle, α.
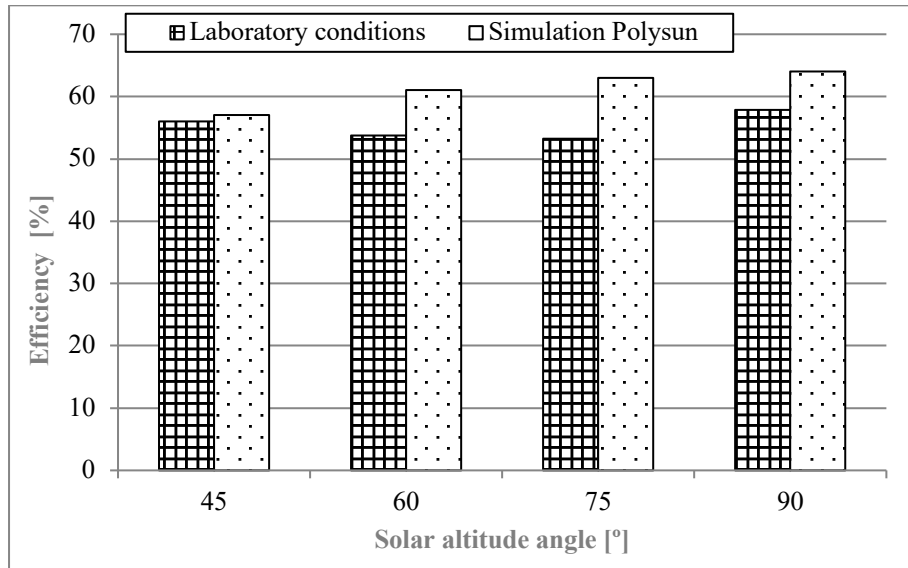

Fig. 10c. PVT collector efficiency under laboratory conditions and corresponding Polysun simulation results
Source: Author's

5. Conclusions

In this study, a PVT collector under field and laboratory conditions was examined. Furthermore, a PVT system was simulated using the demonstration version of *Polysun* software. Through the research, the relationship between orientation of the PVT collector and thermal and electric power generated was investigated. The maximum values of efficiencies for PV module (η_{PV}), solar thermal-collector (η_c) and PVT hybrid collector (η_{PVT}) under different conditions were determined. It was found that the efficiency of the PV module increases with the altitude angle both in laboratory and field experiments. In the case of field experiments, the range of altitude angle was limited (40º;65º). The efficiency of the thermal collector varies slightly in the considered range of altitudes angles and peaks at the lowest considered angle. However, the efficiency of the PV module is more significant overall. Furthermore maximum values of efficiencies for PV, PVT and thermal collector corresponds at the satisfactory level in experiments performed under field and laboratory conditions. The results are in agreement with the earlier reported work on the relation of the tilt angle and efficiencies of PVT modules [21–23]. The simulation results using the *Polysun* software agree reasonably well with experimental data received under laboratory conditions.

Acknowledgments

Nomenclature

A_c	total collector aperture area, m^2
AM	air mass
I_{max}	current point of maximum power, A
I_{mp}	current point of maximum power in standard test conditions, A
I_{sc}	short circuit current, A

I_{rr}	instantaneous solar irradiance, W/m²
k	solar-collector heat-transfer loss-coefficient, W/m² ºC
P_c	instantaneous power of the thermal solar collector, W
P_{max}	maximum nominal power of module, W
PVT	photovoltaic thermal hybrid solar collector,
STC	standard test conditions,
S_e	solar elevation (altitude angle), º
$S_{a30º}$	solar altitude angle for positioning the receiver at angles of 30°, º
$S_{a60º}$	solar altitude angle for positioning the receiver at angles of 60º, º
T_a	ambient temperature, ºC
T_{ab}	average temperature of the absorbing surface, ºC
T_f	fluid temperature at the collector outlet, ºC
T_{inlet}	cooling fluid temperature at the collector inlet, ºC
T_{outlet}	collector outlet temperature, ºC
T_s	water temperature in the storage tank, ºC
Q	energy accumulated in storage tank, kJ
v	wind speed, m/s
V	fluid capacity flow rate during day, m³
V_{max}	voltage on point of maximum power, V
V_{mp}	voltage on point of maximum power in standard test conditions, V
V_{oc}	open voltage, V

Greek Letters

α	angle of incidence, º
βτ	transmittance–absorptance product,
$ε_{sys}$	solar yield, %
ΔT	difference between collector inlet fluid temperature and the ambient air temperature, K
$η_c$	efficiency of solar thermal collector, %
$η_{PV}$	efficiency of the PV module, %
$η_{PVT}$	efficiency of PVT hybrid collector, %

References
[1] M. Lämmle, A. Oliva, M. Hermann, K. Kramer, W. Kramer, PVT collector technologies in solar thermal systems: A systematic assessment of electrical and thermal yields with the novel characteristic temperature approach. Solar Energy, Volume 155, October 2017, Pages 867-879
[2] Proekologiczne odnawialne źródła energii Witold M. Lewandowski 2012.
[3] E. Yandri, The effect of Joule heating to thermal performance of hybrid PVT collector during electricity generation, Renewable Energy, Volume 111, October 2017, Pages 344-352
[4] L.W. Florschuetz, Extension of the Hottel-Whillier model to the analysis of combined photovoltaic/thermal flat plate collectors Sol. Energy, 22 (1979), pp. 361-366
[5] N.Aste, C. Del Pero, F.Leonforte, Water PVT Collectors Performance Comparison, Energy Procedia Volume 105, May 2017, Pages 961-966,
[6] A.H. Besheer, M. Smyth, A. Zacharopoulos, J. Mondol, A. Pugsley Review on Recent Approaches for Hybrid PV/T Solar Technology (2016)
[7] Niccolò Aste, Claudio Del Pero, Fabrizio Leonforte, Massimiliano Manfren, Performance monitoring and modeling of an uncovered photovoltaic-thermal (PVT) water collector, Solar Energy, Volume 135, October 2016, Pages 551-568
[8] Lovedeep Sahota, G.N. Tiwari Review on series connected photovoltaic thermal (PVT) systems: Analytical and experimental studies, Solar Energy, Volume 150, 2017, pp. 96-127
[9] J.S. Coventry Performance of a concentrating photovoltaic/thermal solar collector Sol. Energy, 78 (2005), pp. 211-222,
[10] T.T. Chow, J. Ji, W. He Photovoltaic-thermal collector system for domestic application J. Sol. Energy Eng., 129 (2007), p. 205.
[11] Dupeyrat Patrick, Menezo Christophe, M. Rommel, H. Henning Efficient single glazed flat plate photovoltaic – thermal hybrid collector for domestic hot water system Sol. Energy, 85 (2011), pp. 1457-1468,
[12] www.vitechnology.pl, version 2.01.2016.

[13] www.esrl.noaa.gov, version 2.01.2016.

[14]

[15] http://www.velasolaris.com, version 2.01.2016.

[16] Polysun: User's manual for Polysun 3.3, SPF. Switzerland, 2000.

[17] J. Dąbrowski: Solar collectors to heat water efficiency and profitability of the installation, Publisher University of Life Sciences in Wroclaw, 2009.

[18] S. A. Kalogirou: Progress in Energy and Combustion Science, 30 (2004) p. 231-295,

[19] A. Lisowski: Conversion of renewable energy sources, Publisher Village of Tomorrow, 2009.

[20] Klugman E., Radziemska E., Lewandowski W.M.: Influence of temperature on conversion efficiency of a solar module working in photovoltaic PV/T integrated system, 16th European Photovoltaic Solar Energy Conference and Exhibition, United Kingdom Glasgow, 1-5 May 2000, p. 2406-2409.

[21] Kaya M. Thermal and electrical performance evaluation of PV/T collectors in UAE; 2013.

[22] T.T. Chow, W. He, J. Ji An experimental study of facade-integrated photovoltaic/water-heating system Appl. Therm. Eng. 27 (2007), p. 37–45.

[23] T.T. Chow, A.L.S. Chan, K.F. Fong, Z. Lin, J. Ji Annual performance of building-integrated photovoltaic water-heating system for warm climate application Appl. Energy 86 (2009), p. 689–696.

[24] W. He, X.Q. Hong, X.D. Zhao, X.X. Zhang, J.C. Shen, J. Ji Operational performance of a novel heat pump assisted solar facade loop-heat-pipe water heating system Appl. Energy 146 (2015), p. 371–382.

[25] Subhash Chander, A. Purohit, Anshu Sharma, S.P. Nehra, M.S. Dhaka: Impact of temperature on performance of series and parallel connected mono-crystalline silicon solar cells, Energy Reports 1 (2015) p. 175–180.

[26] R. Tripathi, G.N. Tiwari, Energetic and exergetic analysis of N partially covered photovoltaic thermal-compound parabolic concentrator (PVT-CPC) collectors connected in series. Solar Energy 137 (2016) p. 441–451.

[27] R. Tripathi, G.N. Tiwari, Annual performance evaluation (energy and exergy) of fully covered concentrated photovoltaic thermal (PVT) water collector: An experimental validation Solar Energy 146 (2017) p. 180-190.

[28] Shyam, G.N. Tiwari, Olivier Fischer, R.K. Mishra, I. M. Al-Helal, Performance evaluation of N-photovoltaic thermal (PVT) water collectors partially covered by photovoltaic module connected in series: An experimental study. Solar Energy 134 (2016) p. 302-313.

[29] R. Tripathi, G.N. Tiwari, Energy matrices evaluation and exergoeconomic analysis of series connected N partially covered (glass to glass PV module) concentrated-photovoltaic thermal collector: At constant flow rate mode. Energy Conversion and Management 145 (2017) p. 353-370.

[30] K. Znajdek, M. Sibiński Practical Realization of a Hybrid Solution for Photovoltaic and Photothermal Conversion, Journal of Power and Energy Engineering 7 (2013).

Appendix

As stated in the Introduction, increase in PV module temperature results in a significant efficiency drop. In order to check the impact of temperature on performance of the studied PV, experiments were carried out using a constant light intensity source of 1000 W/m^2 with cell temperature in the range 20-60ºC. From Figs 12a and 12b it is clearly seen that the temperature of the PV module significantly influences the current–voltage characteristic and module efficiency. It was calculated that the forward voltage of the solar cell decreases ~2 mV/K, with temperature increase. The results are in agreement with the earlier data for silicon solar cells [24-29].
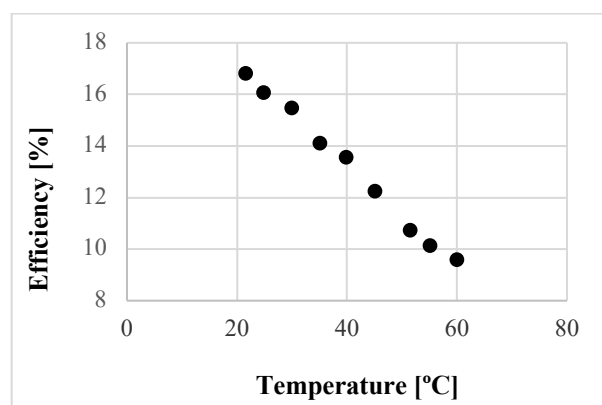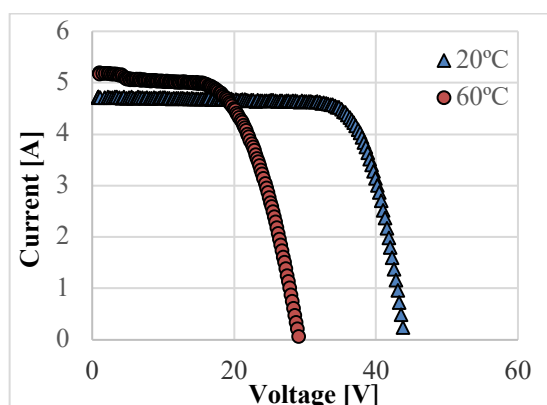
Fig. 11a. The I–V characteristics of PV module under different cell temperatures (20 and 60°C) for light concentration of 1000 W/m^2.
Source: Author's

Fig. 11b. The effect of temperature increase on PV module efficiency for light intensity 1000 W/m^2.
Source: Author's

Figure 11c shows a thermogram of the surface temperature after measurements when the solar thermal system was turned on (left) and off (right).
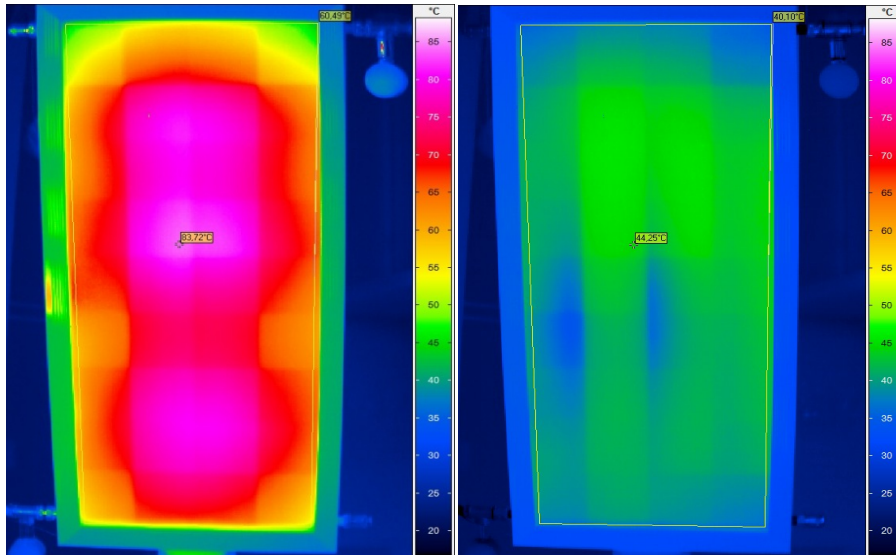

Fig. 11c. Solar hybrid system working without liquid flow (left) solar hybrid system after 15 minutes of liquid flow (right).
Source: Author's

This experiment was conducted at the Department of Semiconductor and Optoelectronic Devices, Lodz University of Technology [30]. Average surface temperature of the solar hybrid system working without liquid flow is ~82 ºC and average surface temperature the same solar hybrid system after 15 minutes of liquid flow is ~42 ºC.